Interface-mode absorption line in ferromagnetic resonance of antiferromagnetically coupled bilayer films: II. Effects of static field configuration and film thickness

1994 J. Phys.: Condens. Matter 6 1155

(http://iopscience.iop.org/0953-8984/6/6/019)

J. Phys.: Condens. Matter 6 (1994) 1155–1176. Printed in the UK

Interface-mode absorption line in ferromagnetic resonance of antiferromagnetically coupled bilayer films: II. Effects of static field configuration and film thickness

Henryk Puszkarski

Surface Physics Division, Physics Institute, A Mickiewicz University, Poznań, Matejki 48/49, Poland 60-769

Received 23 June 1993, in final form 14 October 1993

Abstract. We present a further development of our microscopic theory of the interface spin-wave mode (IM) in exchange coupled bilayer films using the Heisenberg model and including interface inhomogeneity in the spin (exchange, Zeeman and interface uniaxial anisotropy) Hamiltonian. Our theory holds for arbitary (with respect to the film normal) configuration angle ϑ of the film magnetization, arbitrary ferro/antiferromagnetic interface exchange coupling J_i and arbitrary (easy-axis/easy-plane) uniaxial interface anisotropy D_i. Conditions for the occurrence of the IM peak in the bilayer ferromagnetic resonance spectrum are discussed in detail, and a method of resorting to this peak for measuring the interface coupling and pinning anisotropy is proposed. In particular we predict the existence of a critical configuration angle ϑ_c for IM emergence at film magnetization rotation; for antiferromagnetic coupling ϑ_c is a function of the ratio J_i/D_i. Our estimates for real specimens lead to the general conclusion that observation of the IM peak becomes possible already at interface antiferromagnetic exchange coupling of the order of one-hundredth of the exchange bulk coupling.

1. Introduction

In an earlier paper [1] (part I) we proposed the hypothesis that the high-field (HF) line of the double resonance spectrum of a ferromagnetic bilayer film is due to excitation of the interface spin-wave mode, whereas the low-field (LF) line is of bilayer bulk nature. An essential argument invoked by us in favour of this hypothesis was that it naturally leads to the emergence of an inverted pattern of the resonance spectrum, *i.e.* to the experimentally observed pattern with the HF line less intense than the LF line. The analysis of the experimental conditions for the inverted pattern permits their correlation with the conditions predicted by us for the existence of the interface resonance mode—and thus provides a qualitative confirmation of our hypothesis.

The present paper contains a development of our theory of resonance excitation of the interface mode with the aim to permit its *quantitative* experimental verification as well. Hence, the model we shall apply here is more general than that of our earlier work [1–4]: moreover, the interface anisotropy will be postulated in a form permitting the investigation of configurational effects, i.e. ones related with changes in direction of the static magnetic field with respect to the film surface. Within this model, we derive (for the first time in the literature, to our knowledge) formulae enabling us (to a good approximation) to express the interface anisotropy as well as the interface exchange coupling in terms of the resonance characteristics (the resonance intensity and strength of the resonance field) of that line of the ferromagnetic resonance (FMR) spectrum that is due to excitation of the interface mode (IM).

0953-8984/94/061155+22$07.50

This will permit the comparison of the value of the exchange integral of coupling through the interface with the value of the integral obtained from other, independent (non-resonant) measurements, e.g. from hysteresis loop measurements. Thus the theory of the bilayer FMR phenomenon proposed here will permit a complete (both qualitative and quantitative) check of our hypothesis concerning the occurrence of the IM line in the bilayer FMR spectrum.

2. Model

We consider a film consisting of two identical homogeneous ferromagnetic thin layers (sublayers A and B); the two sublayers form a single magnetic system owing to interface exchange coupling. We assume that the externally applied static magnetic field $\boldsymbol{H}_{ex}$ is oriented at some angle with respect to the film normal and can be rotated in the plane perpendicular to the film surface from its perpendicular configuration towards parallel configuration. We assume that the strength of the field lies in a range corresponding to the ferromagnetic resonance conditions; for such values of the field $\boldsymbol{H}_{ex}$ one is justified in assuming that all the spins of the bilayer film are aligned parallel to one another. The effective field acting on a given spin is defined as the sum of the external static field, the uniaxial bulk-anisotropy field and the demagnetization field. Here, to emphasize the interface effects, we neglect the surface-anisotropy fields, but we do include in our considerations the interface-anisotropy fields. We perform our calculations within the framework of the Heisenberg localized-spin model assuming nearest-neighbour exchange interactions and a Zeeman Hamiltonian in standard form. We denote by J_b the bulk exchange integral (between nearest neighbours) and by J^{AB} the exchange integral describing coupling through the interface; we denote by $\mathcal{J}^{AB} \equiv J^{AB}/J_b$ the ratio of the two integrals. We assume the intrinsic interface-anisotropy field (denoted by $\boldsymbol{K}_{int}$) to act on the interface spins of both sublayers, in addition to their bulk effective fields. The above assumption means that we describe the interface anisotropy in a molecular-field approximation, equivalent to neglecting elliptic deformation of the precession cone of the spins at the interface (such deformation intervenes if the interface anisotropy is dealt with in a more rigorous approach). The molecular-field approximation can be conceived to be quite adequate for the description of the spin dynamics since elliptic deformation of interface spin precession, if taken into account, would but insignificantly affect the boundary equations at the interface. The bilayer film thickness (in lattice units) is assumed to be $L - 1 \equiv 2N - 1$, where N is the number of monoplanes in each sublayer. In the following, we shall restrict ourselves to the presentation of results concerning standing spin waves (modes) only. This justifies our taking the magnetic dipole–dipole terms to be negligible for the spin-wave properties (except in giving a static demagnetizing field).

Since our bilayer sample remains symmetric under the operation of reflection with respect to the interface, one obtains spin-wave modes of only two types, namely, symmetric and antisymmetric. The perpendicular wavevector component $k_\perp \equiv k$ is quantized by the following two equations:

$$F(k) \equiv \frac{\cos[\frac{1}{2}(L+1)k]}{\cos[\frac{1}{2}(L-1)k]} = \begin{cases} A_s & (1a) \\ A_a & (1b) \end{cases}$$

where A_s and A_a are *effective* interface pinning parameters for symmetric and antisymmetric modes, respectively. The *intrinsic* interface pinning parameter b (see equations (1) and (2*b*) of paper I [1]) is now redefined as follows:

$$b(m) = 1 - \mathcal{J}^{AB} - \frac{g\mu_B}{2Sz_\perp J_b}[m \cdot \boldsymbol{K}_{int}(m)] \qquad (2)$$

where m is a unit vector in the direction of the static film magnetization (assumed to be homogeneous throughout the film), and $z_\perp$ denotes the number of nearest neighbours in the adjacent plane. It has been established several years ago [5] that the general symmetry properties of the surface/interface spin pinning allow us to express the pinning parameters involved as series expansions in spherical harmonics. In the present model, in accordance with those findings, we can describe the configurational dependence of $b(m)$ on the out-of-plane angle ϑ (the angle between the film magnetization and the normal to the film) by the following expansion:

$$b(\vartheta) = \sum_{l=0}^{\infty} a_l P_l(\cos\vartheta). \tag{3}$$

For further consideration we retain only the first two terms of this expansion since it has already been established that only those terms are relevant in single-layer films [6] when interpreting FMR spectra. The final expressions for the effective interface pinning parameters are given in table 1, where the uniaxial contribution (coming from equation (3)) is denoted by $D_{\rm int}$. The interface exchange coupling $\mathcal{J}^{\rm AB}$ is allowed to take both positive (ferromagnetic) and negative (antiferromagnetic) values, in accordance with recent experimental findings [7–17]. Similarly, the uniaxial interface-anisotropy constant $D_{\rm int}$ is allowed to be either of easy-axis type ($D_{\rm int} > 0$) or easy-plane type ($D_{\rm int} < 0$).

Table 1. Interface pinning parameter A for symmetric (s) and antisymmetric (a) bilayer modes ($k_\parallel \equiv 0$).

$\mathcal{J}^{\rm AB} < 0$	Respective formula	$\mathcal{J}^{\rm AB} > 0$
$A_{\rm a}$	$1 - D_{\rm int}(3\cos^2\theta - 1)$	$A_{\rm s}$
$A_{\rm s}$	$1 - D_{\rm int}(3\cos^2\theta - 1) - 2\mathcal{J}^{\rm AB}$	$A_{\rm a}$

We visualize in figure 1 the k-spectrum arising from equations (1), where the function $F(k)$ is plotted for the bulk modes (in the middle) and for interface modes (to the right for acoustic ($k = it$) and to the left for optical ($k = \pi + it$) ones). On fixing some values of the interface parameters $\mathcal{J}^{\rm AB}$ and $D_{\rm int}$ as well as the configuration of the film magnetization (the angle ϑ), the roots of equations (1) are found by searching for the points of intersection of the respective straight lines ($A_{\rm s}$ for symmetric modes or $A_{\rm a}$ for antisymmetric modes) parallel to the abscissa and curves $F(k)$. It is evident from table 1 that, while all the modes are affected by any change of the angle ϑ or the interface-anisotropy parameter $D_{\rm int}$, a change of the interface coupling $\mathcal{J}^{\rm AB}$ affects only every other mode. Note that for the interface modes the wavenumber k is complex, and that what one finds from the graphs shown in figure 1 are values of its respective imaginary parts t. Henceforth we shall be discussing solely *acoustic* ($k = it$) interface modes.

3. Emergence of interface modes by rotation of the film magnetization

We shall devote the present section to a study of the conditions for the emergence of interface modes when the tilt of the static magnetic field with respect to the film surface is made to vary. The film magnetization follows the field, thus changing the angle ϑ of its orientation with respect to the film normal. Accordingly, we shall be referring to

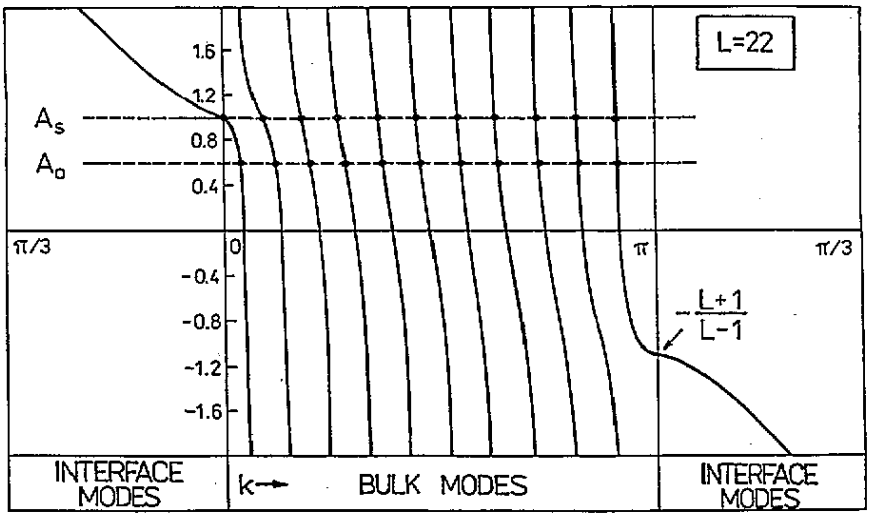

Figure 1. Accessory graph for the discussion of the characteristic equations (1). The roots k corresponding to symmetrical modes are obtained from the points of intersection of the straight line A_s with the curves, while those of the antisymmetrical modes are similarly obtained from the straight line A_a. Bilayer thickness is assumed as 22 monolayers.

these effects as configurational effects. From figure 1, we note that the condition for the existence of the acoustic IM requires that the interface pinning parameters defined in table 1 fulfil the inequality $A > 1$. The imposition of this condition onto A_s and A_a determines the range of angles ϑ for which one (symmetric) or two (symmetric and antisymmetric) IM modes exist at fixed values of the other (interface) parameters. Figure 2 shows the regions of existence of IM in the $\mathcal{J}^{AB}, \vartheta$ plane as determined with the condition $A > 1$, for either of the two possible types of interface anisotropy D_{int}. When analysing the results illustrated in figure 2, let us note that the angle for which the equality $3\cos^2\vartheta - 1 = 0$ holds is a highly specific angle since it defines the only configuration at which the interface anisotropy contributes nothing to the interface pinning and the existence of an IM requires only (as found in our earlier paper [1]) that the interface coupling shall be antiferromagnetic, $\mathcal{J}^{AB} < 0$. Moreover, let us draw attention to the following interplay: in the region where two interface modes exist, one is indebted for its existence to the appropriate value of the interface coupling, whereas the existence of the other is due to the appropriateness of the interface anisotropy values. It is instructive to follow the process of configurational emergence of the two interface modes on the characteristic curves of figure 3 (where only the case $\mathcal{J}^{AB} < 0$ and $D_{int} > 0$ is considered): as the magnetization is made to rotate from the perpendicular configuration ($\vartheta = 0°$) to the parallel configuration ($\vartheta = 90°$), the first to emerge at $\vartheta < 55°$ is the symmetric IM (figure 3(*a*)) and later, at $\vartheta = 55°$, the antisymmetric IM emerges (figure 3(*b*)). At angles $\vartheta > 55°$ the two interface modes coexist and it is noteworthy that the antisymmetric IM is affected by the interface anisotropy D_{int} only; this mode becomes interface-localized at parallel configuration if D_{int} is positive but becomes interface-localized at perpendicular configuration if D_{int} is negative.

Now consider the configurational effects related to the evolution of the two energetically lowest symmetric modes $n = 1$ and 3. These are the modes that govern the inception of the double resonance spectrum in bilayer films because the intensities of the resonance lines corresponding to them are the most significant against the background of the other lines.

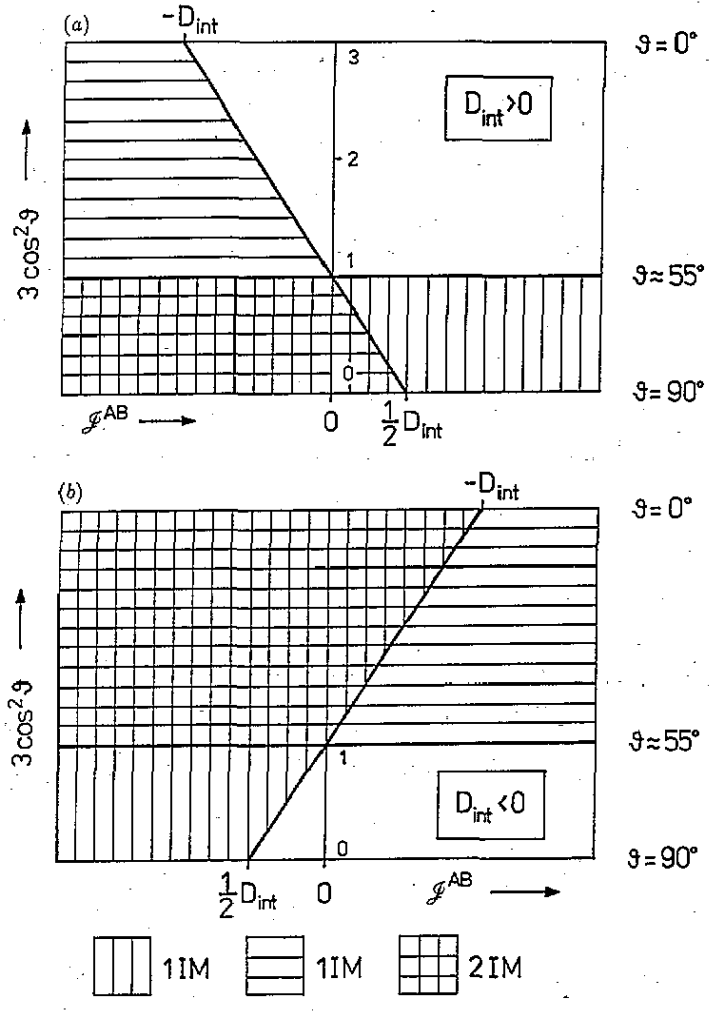

Figure 2. Interface modes exist in a bilayer film only for certain well defined angles ϑ between the film magnetization and the normal to the film surface depending on the type of interface pinning anisotropy D_{int}: (*a*) for easy-axis type, $D_{int} > 0$; (*b*) for easy-plane type, $D_{int} < 0$. Two interface modes exist in the more densely-shaded regions, whereas in the other parts of the shaded regions there exists only one IM.

We start from the case when the bilayer interface is characterized by antiferromagnetic coupling ($\mathcal{J}^{AB} < 0$) and an easy-plane pinning anisotropy ($D_{int} < 0$). In figure 4 we show the profiles of the symmetric modes $n = 1$, 3 and 5 corresponding to this case in their configurationally induced variability with varying ϑ and (in the lower inset) the evolution of the resonance spectrum composed of these modes. Note that the line $n = 1$ corresponds to the IM in the whole range of variability of ϑ and that in the ϑ region close to perpendicular configuration the pattern of the spectrum becomes inverted, $I_3 > I_1$. Now, if we maintain the interface coupling antiferromagnetic but change the interface pinning to easy-axis ($D_{int} > 0$) (see figure 5), the configurational evolution of the profiles and spectra proceeds similarly albeit in the inverse order: now an inverted pattern of the

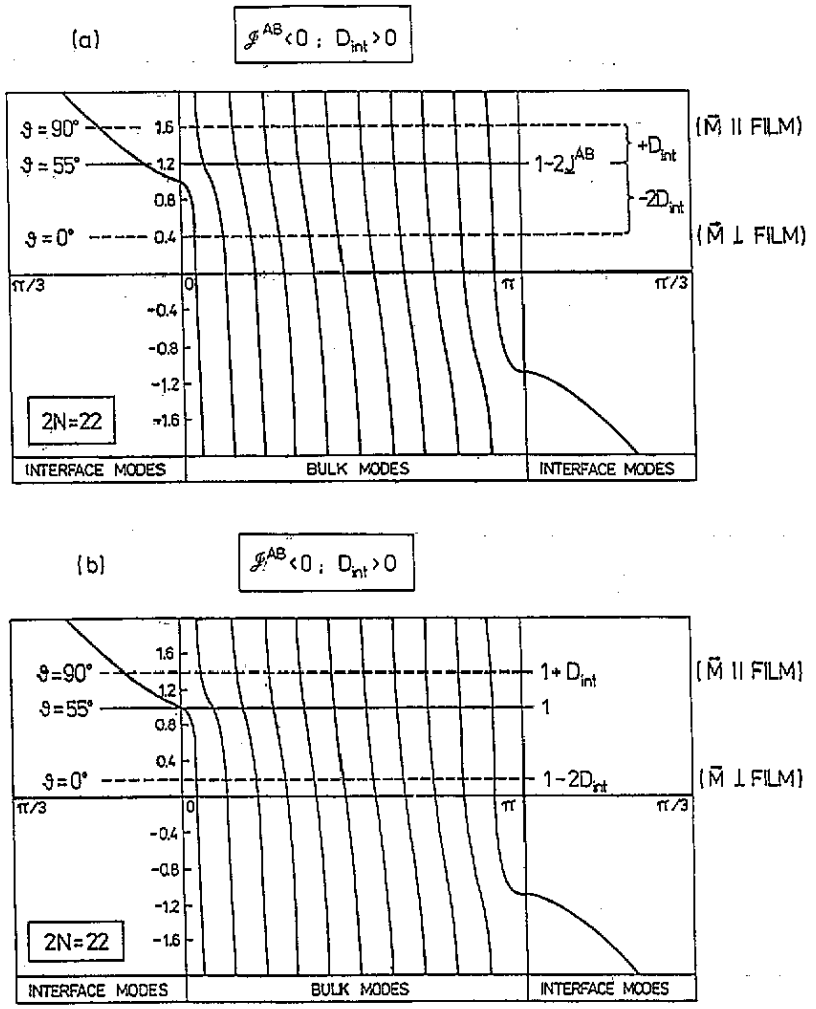

Figure 3. The characteristic curves $F(k)$ are used here to elucidate the emergence of the respective interface mode by way of rotation of the orientation of the film magnetization with respect to the film surface: (*a*) for symmetric mode; (*b*) for antisymmetric mode. For the case considered here it has been assumed that interface exchange coupling is antiferromagnetic and the interface pinning anisotropy is of the easy-axis type. The interface pinning parameters used here are those of table 1. Note that the antisymmetric IM is not affected by the interface coupling.

spectrum appears at angles ϑ close to parallel configuration. Things are quite different if interface coupling is ferromagnetic ($\mathcal{J}^{AB} > 0$; see figures 6 and 7): ferromagnetic coupling makes the achievement of strong interfacial localization of the mode $n = 1$ by varying the configurational angle ϑ more difficult, and an inverted pattern of the spectrum now fails to appear at any of the configurations.

We arrive at very interesting conclusions if, as the quantities for our analysis of the resonance spectrum, we chose the *relative* intensities of the spectral lines—in particular, the ratio of the low-field (LF) line ($n = 3$) intensity and the high-field (HF) line ($n = 1$) intensity. Figures 8 and 9 show the configurational variations of the intensity ratio I_3/I_1 obtained for the combinations possible for positive/negative $\mathcal{J}^{AB}$ and D_{int}. In the case of

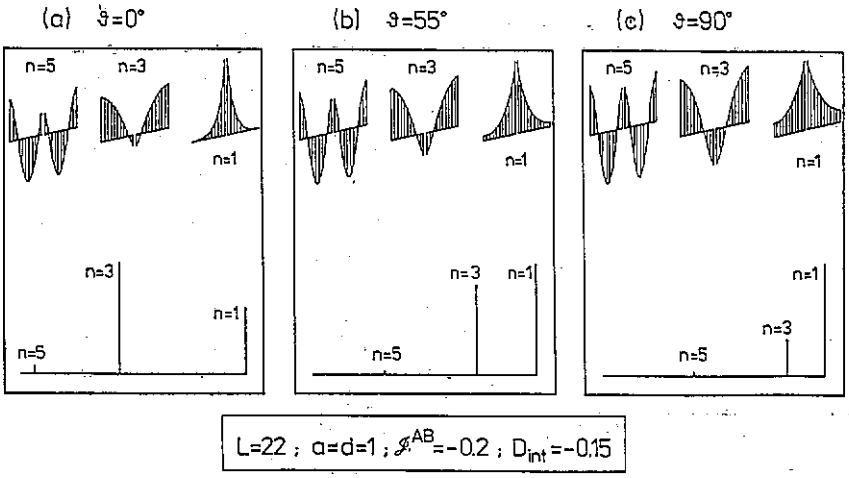

Figure 4. Stick ferromagnetic resonance spectra of the bilayer film calculated for three orientations ϑ of the film magnetization with respect to the film normal for the case when the interface exchange coupling is antiferromagnetic ($\mathcal{J}^{AB} < 0$) and the interface pinning anisotropy is of easy-plane type ($D_{int} < 0$). The calculations are performed for the case when both sublayers A and B have equal thicknesses (11 monolayers each). The units on the horizontal axis are proportional to the normalized energy; peak intensities have also been normalized by assuming the intensity of the highest peak as unity (in each spectrum separately). The profiles of the involved resonant modes ($n = 1, 3, 5$) corresponding to each configuration ϑ are shown in the upper parts of the respective drawings. The surface pinning anisotropies are absent (the respective pinning parameters a and d are equal to unity).

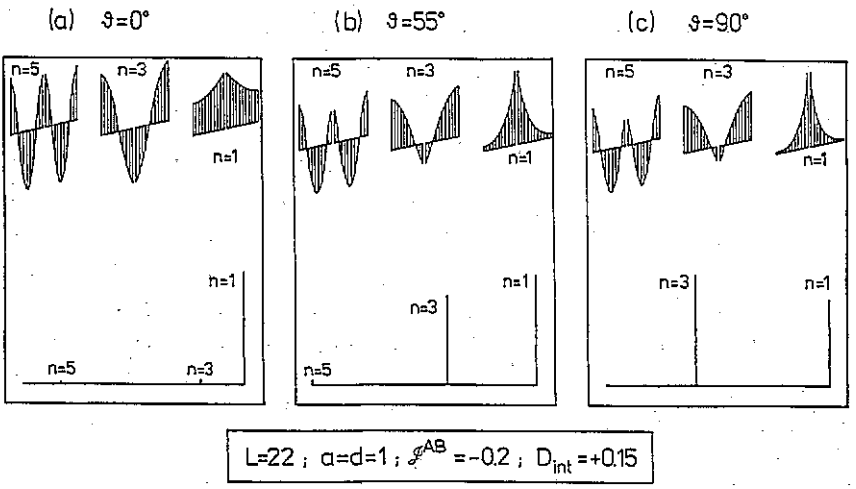

Figure 5. Same as in figure 4 for the case when the interface pinning anisotropy is of easy-axis type ($D_{int} > 0$).

ferromagnetic interface coupling (figure 8) the configurational variations of I_3/I_1 exhibit a critical angle effect: at a certain value of ϑ the resonance spectrum becomes single-peak—for this particular value of ϑ the ratio $I_3/I_1 \equiv 0$ (see also figure 7). The critical

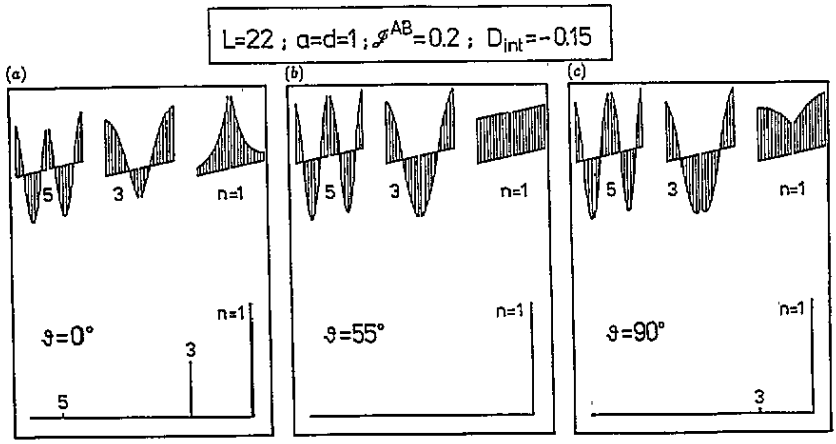

Figure 6. Same as in figure 4 for the case when the interface coupling is ferromagnetic ($\mathcal{J}^{AB} > 0$) and interface pinning is of easy-plane type ($D_{int} > 0$).

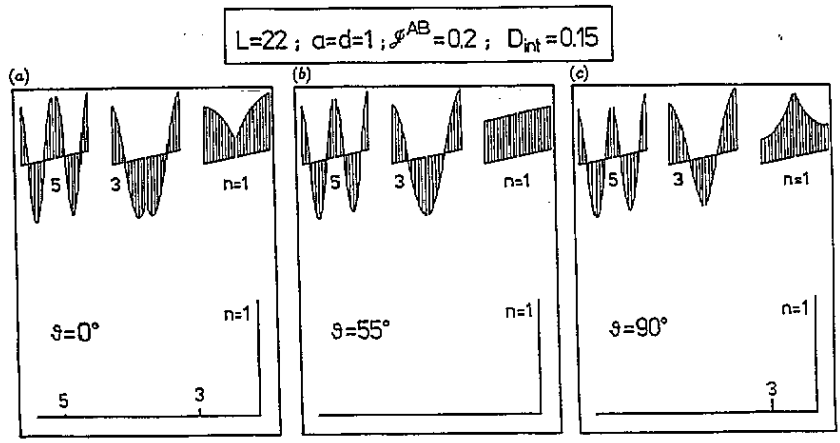

Figure 7. Same as in figure 6 for the case when the interface pinning anisotropy is of easy-axis type ($D_{int} > 0$).

resonance spectrum always consists of but one resonance line, corresponding to excitation of the uniform mode $k = 0$; this, consequently, requires the fulfilment of the condition $A \equiv 1$. Thus, with regard to table 1, the critical angle amounts to $\vartheta_c = 55°$ in the case of ferromagnetic interface coupling. In the antiferromagnetic case ϑ_c is determined by the condition

$$(3\cos^2\vartheta_c - 1)D_{int} = -2|\mathcal{J}^{AB}| \tag{4}$$

and is no longer a constant but is dependent on the interface parameters; in particular, if the latter are chosen appropriately (see figure 9), the system can fail to exhibit a critical angle. There is yet another property that distinguishes the cases of ferro- and antiferromagnetic coupling: in the latter case there exists another specific angle for which $I_3/I_1 \equiv 1$ above which the regular pattern of the spectrum goes over into the inverted pattern (or vice versa). The occurrence of such an angle in the case of ferromagnetic coupling is unlikely with

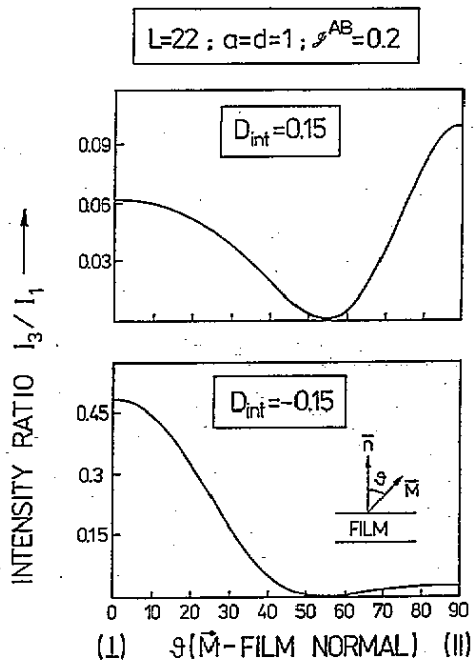

Figure 8. Intensity ratio of the low-field ($n = 3$) and high-field ($n = 1$) lines of the bilayer-film resonance spectrum (versus the configuration angle ϑ of the film magnetization) calculated for the case of ferromagnetic interface exchange coupling.

regard to the very low intensities obtained for the bulk modes in this case. As a rule, the equality $I_3 = I_1$ holds only if the HF line corresponds to IM excitation.

Let us now consider the configurational dependence of the *position* of the resonance lines. This will lead us to a simple criterion enabling us to identify the type of pinning anisotropy at the interface. Figure 10 shows how the reduced energies of the modes expressed in terms of $\cos k$ vary with the angle ϑ (for the sake of completeness we have included the antisymmetric modes $n = 2$ and 4 although they do not participate in the resonance). These reduced energies provide a good reproduction of how the positions of the lines of the experimental resonance spectra behave if reduced to a single common scale on which the resonance field H_{unif} corresponding to hypothetical ordinary FMR occupies an invariant position throughout the whole range of variability of ϑ. Now figure 10 shows convincingly that on performing this reduction we find that the resonance positions unequivocally exhibit a tendency to shift towards *higher* fields for interface anisotropy pinning of the easy-axis type ($D_{int} > 0$) and towards *weaker* fields for easy-plane type pinning ($D_{int} < 0$) irrespective of whether the interface exchange coupling is ferromagnetic or antiferromagnetic.

4. Ferromagnetic resonance intensity equalization effect

The previous section has introduced the proof that *equalization* of the resonance intensities of the HF and LF lines of the spectrum can take place only if the lines correspond to excitation of modes differing as to their nature: the HF line has to be of interface-mode (IM)

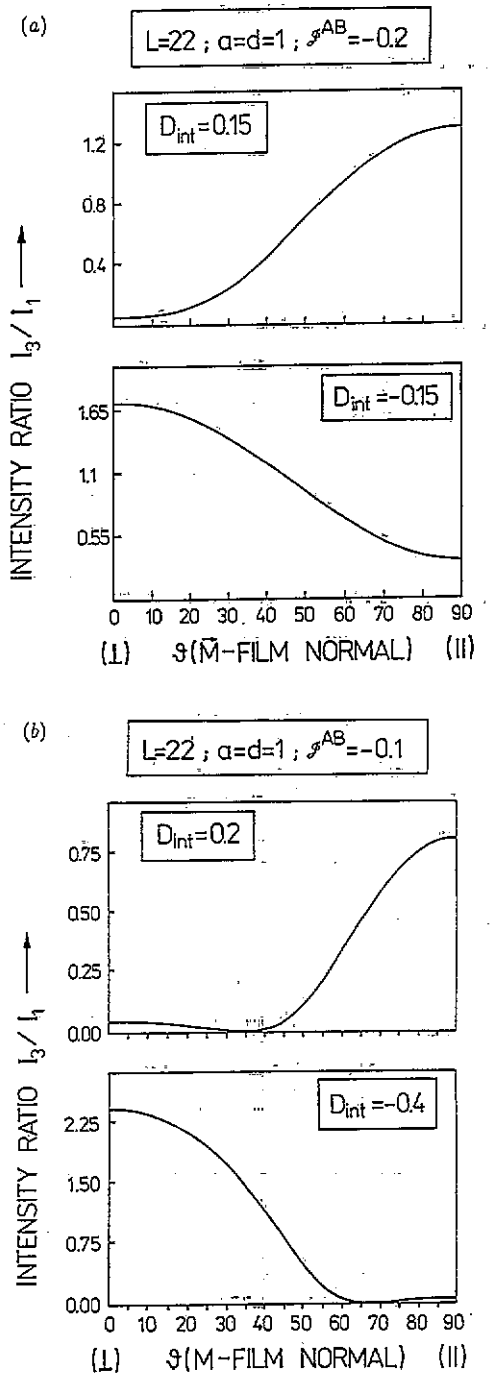

Figure 9. Same as in figure 8 for antiferromagnetic interface exchange coupling ($\mathcal{J}^{AB} < 0$).

type whereas the LF line has to be of bulk-mode (BM) type. Figure 11 shows typical shapes of the two (HF and LF) excited lines and figure 12 visualizes the essential interdependence of their profiles residing in the fact that an increase in localization of the IM is correlated

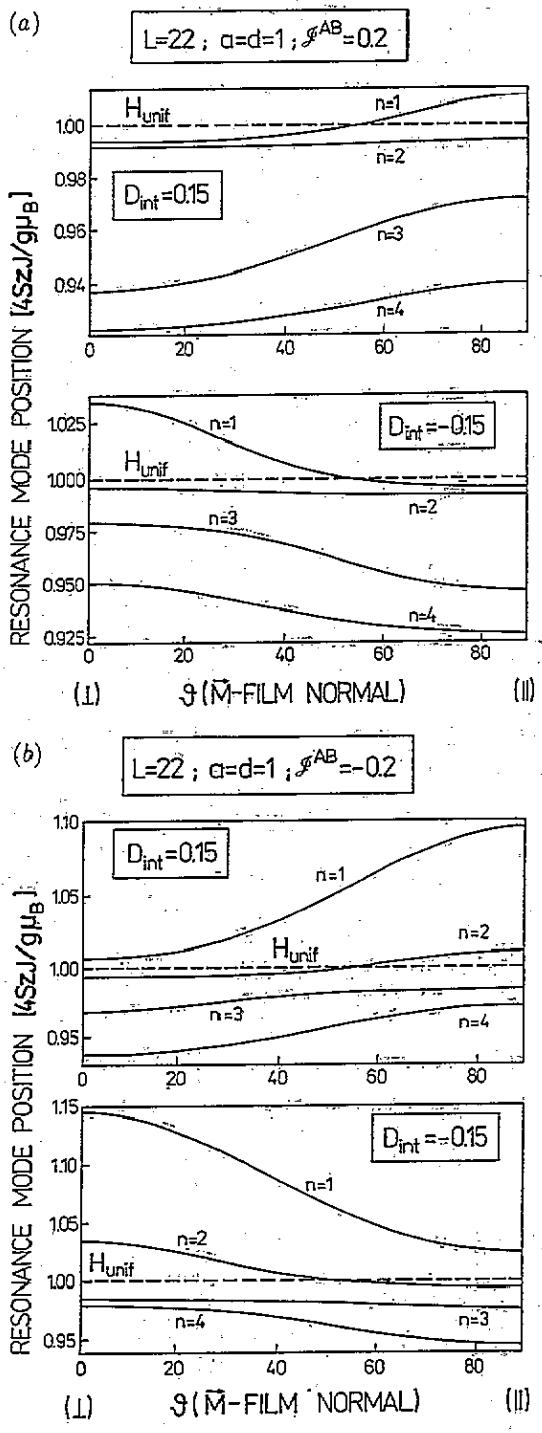

Figure 10. Bilayer spin-wave mode energies (simply: $\cos k$) versus the configurational angle ϑ of film magnetization (n labels the modes) for the case of (a) ferromagnetic and (b) antiferromagnetic interface exchange coupling $\mathcal{J}^{AB}$ and different types of interface pinning anisotropy (D_{int}). Note that the energy is scaled in such a way that the position of the hypothetical uniform mode remains unchanged with varying angle ϑ.

with a simultaneous shift of the nodes of the BM towards the interface. Moreover we keep in mind that the existence of a symmetric IM requires that the respective interface pinning parameter shall fulfil the inequality $A_s > 1$ (in this section, for brevity, we shall be writing A in place of A_s).

Inserting $k = it$ (t is the localization increment of the IM) into equation (1*a*) we obtain the following equation:

$$\frac{\cosh[\frac{1}{2}(2N+1)t]}{\cosh[\frac{1}{2}(2N-1)t]} = A \tag{5}$$

which we solve in the following approximation (see [18]):

$$e^{-2Nt} \ll 1. \tag{6}$$

The inequality (6) is satisfied if $N \gg 1$. In this approximation, equation (5) yields

$$e^t = A. \tag{7}$$

On the other hand, the IM amplitude can be expressed as a function of the localization increment in the form $e^{-|r|t}$, where r measures the distance from the interface in lattice units across the film (see figure 11). Finally, the *normalized* amplitudes of the IM can be expressed explicitly in terms of the interface pinning parameter A as follows:

$$u_{IM}(r) = \frac{1}{\sqrt{2}}\left(\frac{A^2-1}{A^2-A^{-2(N-2)}}\right)^{1/2} A^{-|r|} \qquad \text{(interface mode, } n=1\text{).} \tag{8}$$

To derive the respective formula for the bulk mode $n = 3$ we adopt an approximation that resides in *linearization* of its amplitude across the bilayer film. In this approximation we use the formula (4.14) of [6] allowing us to express the respective ($n = 3$) mode amplitude by the interface pinning parameter A. However, when performing this linearization, we have to take care to preserve the proper location of the nodes specific for the *bilayer* mode, as indicated in figure 12. The formula thus obtained for the normalized amplitudes reads as follows:

$$u_{BM}(r) = \left(\frac{3}{2N}\right)^{1/2}[1+N(A-1)+N^2(A-1)^2]^{-1/2} \times\left[1-|r|\left(A-1+\frac{2}{N-1}\right)\right] \qquad \text{(bulk mode, } n=3\text{).} \tag{9}$$

The two formulae (8) and (9) jointly provide a very good picture of the mutual correlation holding between the increase in strength of the IM localization and the simultaneous shift of the nodes of the BM towards the interface, as shown in figure 12.

The intensity of the resonance line is proportional to the squared sum over the respective mode amplitudes across the bilayer film. Using the formulae (8) and (9) we obtain for the IM and BM lines, with accuracy to the same omitted constant factors,

$$I_{IM} \sim 2\frac{A+1}{A-1}\frac{A-A^{-(N-2)}}{A+A^{-(N-2)}} \tag{10}$$

$$I_{BM} \sim \frac{3}{2}\frac{(A-1)N^2}{1+(A-1)N} \tag{11}$$

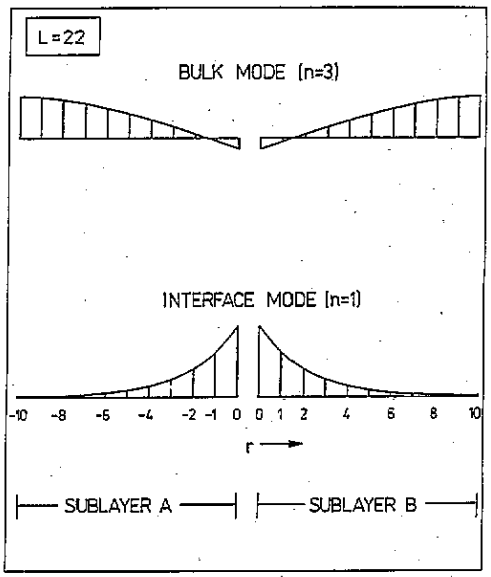

Figure 11. Accessory graph for the derivation of the formulae (8) and (9) expressing the amplitudes of the two energetically lowest bilayer symmetrical modes (when the respective interface pinning parameter A_s is greater than unity).

permitting the determination of the intensity ratio R as

$$R \equiv \frac{I_{BM}}{I_{IM}} = \frac{3}{4}\frac{(A-1)^2}{A+1}\frac{N}{A-1+1/N}\frac{A+A^{-(N-2)}}{A-A^{-(N-2)}}. \tag{12}$$

In order to get some idea of the range of validity of equation (12) we have plotted in figure 13 the *strict* dependence of R on N obtained by numerical computation: we thus find that equation (12) is applicable only in the range of (great) N values where the function $R(N)$ is strictly or almost linear (in figure 13 this occurs for $N > 15$). For a very great N we may neglect in equation (12) the contribution from the last factor (the one containing N in the exponent). This leads us to the following, still simpler expression:

$$R \simeq \tfrac{3}{4}N(A-1)^2/[(A+1)(A-1+1/N)] \tag{13}$$

whence we easily derive the interface pinning parameter A as a function of the intensity ratio R and the film thickness L ($\equiv 2N$):

$$A = 1 + [R + (R^2 + \tfrac{3}{2}R)^{1/2}]/(\tfrac{3}{8}L - R). \tag{14}$$

Thus, we see that the experimental measurement of the intensity ratio R and, more particularly, the experimental observation of the equalization effect ($R = 1$) provides a direct *quantitative* method for the determination of the interface pinning characteristics on the basis of equation (14).

In the next section we shall give an assessment of the accuracy up to which the approximate formula (14) enables us to determine the interface exchange coupling.

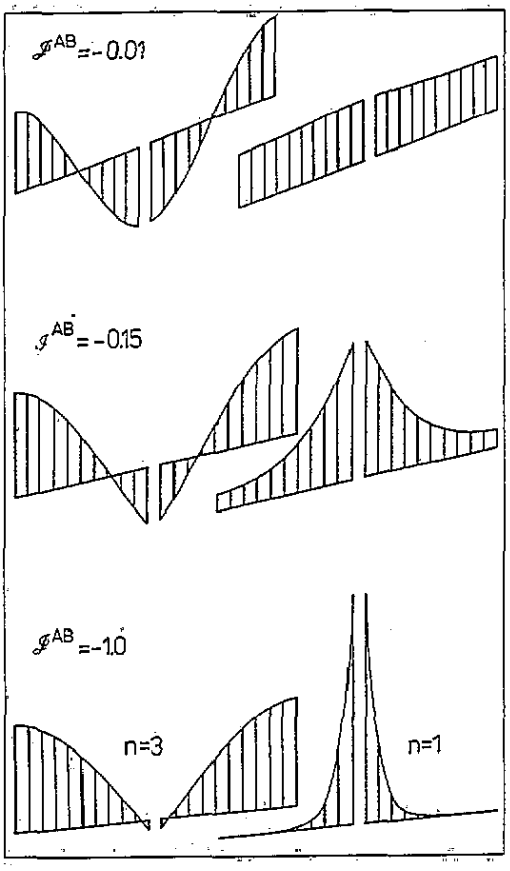

Figure 12. The two energetically lowest symmetrical modes in their dependence on the value of the antiferromagnetic interfacial exchange coupling (the case with $D_{int} = 0$). Note the correlation between the strength of the localization of the interface mode and the location of the nodes of the bulk mode.

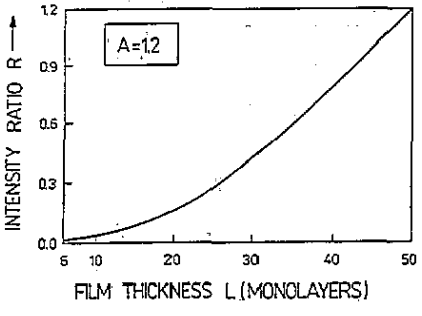

Figure 13. Numerically determined exact values of the intensity ratio of the (HF) interface-mode line and the (LF) bulk-mode line versus the bilayer film thickness. The film thickness $L \equiv 2N$ monolayers, and the (symmetrical) interface pinning parameter value is set at $A_s = 1.2$.

5. Ferromagnetic resonance spectrum dependence on bilayer film thickness

In this section we shall restrict ourselves to considering the perpendicular configuration ($\vartheta = 0°$) and shall assume that uniaxial interface anisotropy is absent ($D_{int} = 0$). The effective interface pinning parameters for the case under consideration are assembled in table 2. Figure 14 shows the computed FMR spectrum in its evolution with varying film thickness L. Since we have chosen the interface coupling as antiferromagnetic, the first line of the spectrum corresponds to the IM and the second line to the BM. A highly characteristic feature of this evolution resides in the fact that the position of the IM is practically independent of the film thickness, whereas the BM line tends to a position corresponding to the uniform mode (UM). The change in the relative intensities of the two lines accompanying the variations in L is interpreted in figure 15, where we note that with growing L the strength of the IM localization increases and is accompanied by a shift of the nodes of the BM profile towards the interface.

Table 2. Interface pinning parameter A for symmetric (s) and antisymmetric (a) bilayer modes ($M \perp$ film).

$\mathcal{J}^{AB} < 0$	Respective formula	$\mathcal{J}^{AB} > 0$
A_a	$1 - 2D_{int}$	A_s
A_s	$1 - 2(D_{int} + \mathcal{J}^{AB})$	A_a

Work on these film thickness effects appears to be a promising field of research since—as predicted by equation (13)—the relation between the intensity ratio R and the film thickness L should be linear. If experiment confirms this linearity, equation (14) leads us to the following formula for the interface exchange coupling integral $\mathcal{J}^{AB}$:

$$\mathcal{J}^{AB} = -[R + (R^2 + \tfrac{3}{2}R)^{1/2}]/(\tfrac{3}{4}L - 2R). \tag{15}$$

As an example, in table 3 we give the values of $\mathcal{J}^{AB}$ calculated with equation (15) for different values of R and L and, for comparison, the exact numerical results. One notes that the results obtained for $\mathcal{J}^{AB}$ with equation (15) are the better the greater are R and L.

Table 3. Calculated values of antiferromagnetic (negative) interface exchange coupling $\mathcal{J}^{AB}$ for different intensity ratios.

Intensity ratio $R = I_{BM}/I_{IM}$	$R = 0.5$			$R = 1$			$R = 2$			$R = 4$		
Film thickness L (monolayers)	10	20	40	10	20	40	10	20	40	10	20	40
$\lvert\mathcal{J}^{AB}\rvert$ Exact value	0.415	0.170	0.078	0.691	0.257	0.114	1.720	0.466	0.188	—	1.240	0.384
Equation (12)	0.222	0.105	0.051	0.454	0.192	0.089	1.320	0.421	0.149	—	1.234	0.393

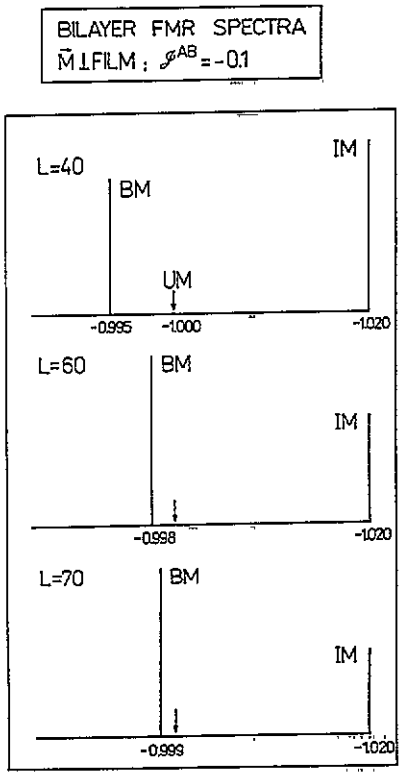

Figure 14. Stick FMR bilayer spectra (for perpendicular configuration) calculated for various film thicknesses, for the case of antiferromagnetic interfacial coupling $\mathcal{J}^{AB} = -0.1$. The horizontal axis corresponds to the normalized energy (i.e. $\cos k$). IM means interface mode and BM bulk mode, and the position of the hypothetical uniform mode is marked as UM.

6. The position of the interface mode versus the interface parameter

Here, too, we shall consider the perpendicular configuration ($\vartheta = 0°$) only. The bulk spin-wave mode energy, expressed in terms of the wavenumber k, is, in this case, given by the following formula:

$$E(k) = 4SJ_b z_\perp (1 - \cos k) + g\mu_B (H + H_a - 4\pi M) \tag{16}$$

where the effective field acting on a given spin is expressed as the sum of the external static field H, the uniaxial bulk-anisotropy field H_a and the demagnetization field $-4\pi M$. Obviously, k is quantized by equations (1) with the respective pinning parameters defined as in table 2. For interface modes $k = it$, and in equation (16) the trigonometric cosine should be replaced by the hyperbolic cosine; simultaneously, equations (1) read

$$\frac{\cosh[\frac{1}{2}(L+1)t]}{\cosh[\frac{1}{2}(L-1)t]} = \begin{cases} A_s & (17a) \\ A_a. & (17b) \end{cases}$$

It will prove convenient to make use of the *reduced* energy, expressed simply by $\cos k$ for bulk modes and $\cosh t$ for interface modes. The reduced energy determines (with accuracy to a constant) the position of the resonance field in units $4SJ_b z_\perp / g\mu_B$.

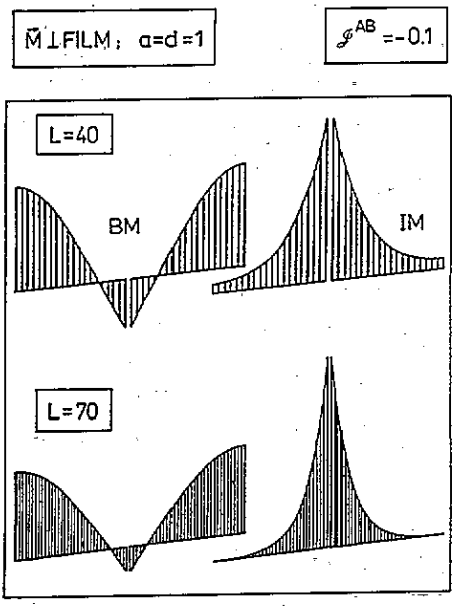

Figure 15. Profiles of the modes associated with the resonance lines depicted in figure 14.

Figure 16 shows the reduced energies of the resonance modes (IM and BM) in their dependence on the interface coupling and the bilayer film thickness, on the simplifying assumption of $D_{\text{int}} = 0$. For comparison, the energy level corresponding to the resonance field of the *uniform mode* (UM) is also indicated in figure 16; it will be kept in mind that since the position of the UM corresponds to $k = 0$ exactly, the UM occurs in the spectrum only if the necessary boundary conditions are fulfilled. Therefore, what we call 'the UM position' represents no more than a point of reference on the scale of the spectrum. Noteworthy are the following characteristic features of the graphs: (i) the separation between the positions of the modes IM–BM is much more sensitive to changes in film thickness than to changes in interface coupling: whereas, on the contrary, (ii) the separation IM–UM is essentially sensitive to changes in $\mathcal{J}^{AB}$ only. This is why we propose to use (rather than the separation of the two resonance lines) the separation IM–UM for the determination of the interface characteristics.

Equation (17) is solvable in the approximation to $L \gg 1$ (see [18]). We then obtain, as in section 4, $e^l = A$, enabling us to express the energy of the interface mode in the following form:

$$E_{\text{IM}}(A) = 2SJ_b z_\perp (2 - A - 1/A) + g\mu_B(H_{\text{IM}} + H_a - 4\pi M) \tag{18}$$

whence

$$\delta H \equiv (H_{\text{IM}} - H_{\text{UM}})g\mu_B/(2SJ_b z_\perp) = A + (1/A) - 2 \tag{19}$$

and, finally,

$$A = 1 + \delta H + [(\delta H)^2 + 2\delta H]^{1/2}. \tag{20}$$

Equation (20) enables us to calculate the value of the effective interface pinning parameter A from the separation of the positions of the IM and UM; it is worth noting that to this aim

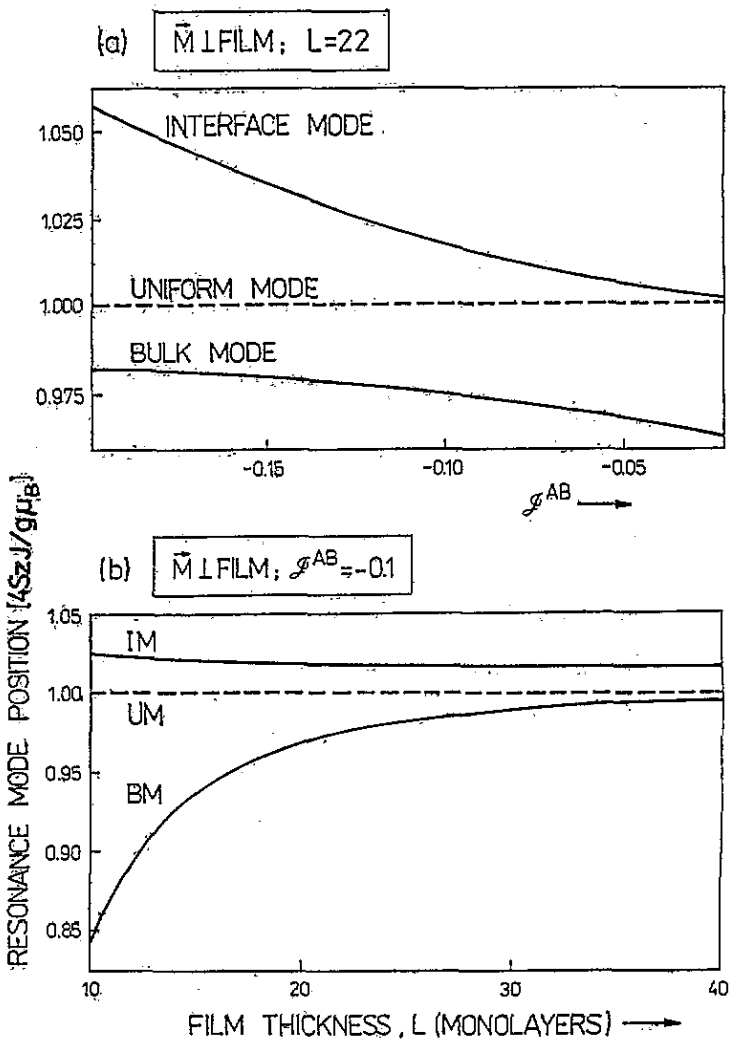

Figure 16. Numerically calculated positions of the bilayer FMR lines (IM interface mode, BM bulk mode) versus (*a*) the interfacial coupling $\mathcal{J}^{AB}$ and (*b*) the film thickness L, for the case $D_{int} = 0$ (i.e. no intrinsic interface anisotropy). The ordinate axis is scaled in dimensionless units of the reduced energy (simply: $\cos k$).

equation (20) is applicable both for symmetric and antisymmetric IM (obviously, A now stands for A_s or, respectively, A_a).

It should moreover be noted that figure 16 provides us with a straightforward criterion for the identification of the IM line in the bilayer FMR spectrum by varying the thickness of the bilayer film: in the range of great thickness L its position is practically insensitive to variations in L, whereas in that of intermediate L it shifts towards *stronger* fields with decreasing L while the BM line shifts towards weaker fields.

7. Experimental implications

Let us discuss briefly the typical FMR experiment performed in bilayer films. Heinrich *et al* [19] studied the FMR spectra obtained in ultrathin well defined bilayers of Fe(001)/Cu(001)/Fe(001) with Cu thicknesses ranging between 6 and 12 monolayers (ML). Moreover they performed supplementary measurements on Fe/Cu and Cu/Fe single-layer films, where the Fe layers were respectively 5 to 10 ML thick, i.e. the same as in their bilayer samples. Their results can be summarized as follows:

(i) the single-layer Fe films always showed but one resonance peak, with positions differing between the two control samples because of the differences in their perpendicular uniaxial anisotropies;

(ii) also those bilayer films where the Cu interlayer thickness d_{Cu} was less than 9 ML showed but one resonance peak;

(iii) all bilayers with $d_{Cu} > 9$ ML, on the other hand, exhibited two resonance peaks in FMR, the weaker peak always being located at the high-field side of the spectrum.

Independently of FMR, other studies by the same authors showed that in weak external fields the magnetizations of the two Fe sublayers were parallel if the interlayer thickness d_{Cu} was less than 9 ML and antiparallel if $d_{Cu} > 9$ ML, suggesting that the magnetic coupling in (Fe/Cu/Fe) bilayers changes from ferromagnetic to antiferromagnetic when the Cu interlayer thickness reaches $\simeq 9$ ML. This allows the authors to conjecture that the weaker resonance peak is of 'optical' nature, i.e. (in accordance with the authors' terminology) corresponds to the mode in which RF magnetizations oscillate out of phase, whereas the remaining (stronger) peak is of acoustic nature.

Our microscopic theory also (though differently) explains *all three* (listed above) characteristic features of the experimentally observed FMR spectra. We come to the conclusion, however, that both the HF and LF resonance peaks observed in (Fe/Cu/Fe) bilayers are *acoustic* in nature, i.e. they correspond to modes whose RF magnetizations oscillate in phase, but differ in that the weaker peak corresponds to the mode that is localized at the interface ('interface mode') whereas the stronger peak is *spatial* in nature ('bulk mode'). Precisely, the strict precondition for the existence of an interface-localized mode resides in the emergence of antiferromagnetic coupling through the interface between the sublayers; this explains why it exists in the FMR spectrum as an additional peak only in those samples where $d_{Cu} > 9$ ML.

With a view to experimental measurements on *real* systems, it may now be of interest to calculate the interface parameters (resulting from our theory) necessary for the occurrence of the IM in their spin-wave resonance (SWR) spectrum and, particularly, for the equalization effect ($R = 1$) to set in. With this in mind we shall derive a formula enabling us to express our microscopic (dimensionless) interface pinning parameter A in terms of the *macroscopic* measure of interface pinning energy E_{int} generally used by the experimentalists, i.e. the energy of all interface spins present per unit area (erg cm^{-2}). Similarly as the surface pinning energy E_{surf} is expressible in terms of the surface pinning parameter (see [18]), the interface pinning energy can be expressed in terms of the interface parameter A as follows:

$$E_{int} = S^2 z_\perp J_b a_0^{-2} (A_{int} - 1) \tag{21}$$

with a_0 the lattice constant. On the other hand, with regard to the dispersion law (equation (16)), the resonance condition for perpendicular field orientation takes the form:

$$(\omega/\gamma) = (4SJ_b z_\perp/g\mu_B)(1 - \cos k) + (H + H_a - 4\pi M) \tag{22}$$

or, in the long-wavelength approximation ($k \simeq 0$),

$$(\omega/\gamma) = (2A_{ex}/M)(k/a_0)^2 + (H + H_a - 4\pi M) \tag{23}$$

where M is the bulk film magnetization, and the exchange stiffness constant A_{ex} is expressed by the microscopic quantities as follows:

$$A_{ex} = SJ_b z_\perp M a_0^2/g\mu_B \equiv S^2 J_b z_\perp a_0^{-1}. \tag{24}$$

This allows us to replace (21) by the following formula:

$$E_{int} = A_{ex} a_0^{-1}(A_{int} - 1). \tag{25}$$

Likewise, we reinterpret the quantity δH, given *microscopically* by equation (19), in terms of the *macroscopic* quantities as follows:

$$\delta H \equiv (H_{IM} - H_{UM})(M/2A_{ex})a_0^2. \tag{26}$$

We shall now make an estimate for a material with magnetic properties close to those of Permalloy $Ni_{80}Fe_{20}$. This amounts to the assumption of $a_0 = 3$ Å, $A_{ex} = 1.0 \times 10^{-6}$ erg cm^{-1} and $4\pi M = 8.5$ kG. Assuming that the IM peak is distant from the UM position by 10^3 G, and on applying equation (19), we arrive at $\delta H \simeq 3 \times 10^{-4}$ which, with equation (20), gives the value of the interface parameter required, namely $A_{int} = 1.025$. Moreover if we require that equalization of the resonance intensities, $R = 1$, shall take place for $A = 1.025$, we get with equation (14) a value of $L \simeq 250$ ML for the film thickness, which is equivalent to about 2×400 Å and lies well within the thin-film range. On the other hand, our estimate of the interface parameter value involves an interface energy of

$$E_{int} = \tfrac{1}{3}(A_{int} - 1) \times 10^2 \text{ erg cm}^{-2} \simeq 0.83 \text{ erg cm}^{-2} \tag{27}$$

well within the range of energies measured in experiments on *real* magnetic films.

Throughout the present work, aimed at an illustration of the resonance effects related to the existence of IM, we used A values considerably in excess of that obtained above (as required for *real* specimens). Obviously, we were led to proceed along these lines because our numerical computations were carried out for a film with a thickness of as little as $L = 22$ ML. By equation (14), a film as thin as that requires an A value much greater than for a film one order of magnitude thicker, to obtain the same equalization effect (strictly, a difference of one order of magnitude in the film thickness involves a similar change in the value of $(A - 1)$ which, as well, results from equation (14)).

We shall now estimate the value of the interface coupling exchange integral $\mathcal{J}^{AB}$ for the situation considered above. For the sake of simplicity, we shall assume $D_{int} \equiv 0$, leading to $A_{int} \equiv 1 - 2\mathcal{J}^{AB}$. The reader who has gone through our preceding estimates is now well aware that the only significant contribution to A, equation (20), comes from the term in $2\delta H$. Thus, we are justified in writing

$$A_{int} = 1 + (2\delta H)^{1/2}. \tag{28}$$

With regard to (26), this leads to

$$A_{int} = 1 + a_0[(M/A_{ex})(H_{IM} - H_{UM})]^{1/2} \tag{29}$$

and, by (25), we get

$$E_{\text{int}} = [M A_{\text{ex}}(H_{\text{IM}} - H_{\text{UM}})]^{1/2} \tag{30}$$

and

$$J^{\text{AB}} = -(a_0/2)[(M/A_{\text{ex}})(H_{\text{IM}} - H_{\text{UM}})]^{1/2} J_{\text{b}}. \tag{31}$$

With $H_{\text{IM}} - H_{\text{UM}} = 10^3$ G for Permalloy, we find $J^{\text{AB}} = -0.0125 J_{\text{b}}$ and arrive at the value of $E_{\text{int}} = 0.83$ erg cm^{-2} calculated above. We now evaluate these quantities for Fe assuming $4\pi M = 21.5$ kG, $a_0 = 2.86 \times 10^{-8}$ cm and $A_{\text{ex}} = 2.09 \times 10^{-6}$ erg cm^{-1}. With equations (30) and (31) we obtain, respectively, $J^{\text{AB}} = -0.0116 J_{\text{b}}$ and $E_{\text{int}} = 1.90$ erg cm^{-2}, leading to an interface parameter value very close to that obtained for Permalloy (Py): $A_{\text{int}} = 1.023$.

The preceding estimates incline us to the general conclusion that the observation of the IM peak becomes possible already at an interface exchange coupling of the order of one-hundredth of the exchange bulk coupling (and all the more so at greater values). As probably the best candidate fulfilling the above conditions we see Fe/Cr/Fe bilayers, where interface coupling is antiferromagnetic over a range of thickness of Cr (estimated at 5 Å $< d_{\text{Cr}} <$ 30 Å). In fact, in the literature available to us we have come upon an unpublished work by Bosse [20] where we identify the IM peak in the SWR spectra obtained in his experimental work on Fe/Cr/Fe bilayer films. Noteworthy in this respect are figures 6.20 and 6.24 of Bosse's work [20] giving his SWR measurements for $Fe_{120}/Cr/Fe_{120}$ with variable Cr thickness (the thickness of the Fe sublayers amounted to 120 Å each). Bosse estimates that antiferromagnetic interface coupling was the strongest at $d_{\text{Cr}} = 8$ Å, for which value of the Cr thickness the FMR spectrum showed an inverted pattern (i.e. $R > 1$), with a separation of $\Delta H_{12} \simeq 10^3$ G. His value reported for the 'interface coupling energy' is $A_{12} \simeq 0.5$ erg cm^{-2} (Bosse's definition of the interface energy corresponds to our $\frac{1}{2}E_{\text{int}}$) and is in the range of our estimate of 0.95 erg cm^{-2}. At the time of his measurements, Bosse [20] obviously did not interpret the high-field line observed by him as being due to IM excitation. This, at present, appears to us to be its true interpretation, as resulting from our theoretical predictions.

Also, the latest, as yet unpublished measurements by Hurdequint and co-workers [21] on the system $Py/Al_2O_3/Py$ appear, in our opinion, to exhibit the presence of the IM peak. However, maybe a still better candidate of a system based on Permalloy for studies on the IM peak can be Py/Cu/Py in a range of Cu thickness where interface coupling is antiferromagnetic. Also, Bosse [20] carried out SWR measurements on such a Permalloy–copper system for different configurations of the angle ϑ (see figure 6.3 of [20]) and determined a critical angle $\vartheta_{\text{c}} = 82.8°$ in $Py_{300}/Cu_{50}/Py_{300}$. This result, when confronted with our formula (equation (4)), shows that Bosse's bilayer fulfils the relation $D_{\text{int}} \simeq 2.1 \mathcal{J}^{\text{AB}} < 0$, leading us to the conclusion that the IM peak is present in the SWR spectra obtained for configurations with $\vartheta > \vartheta_{\text{c}}$. (The possible source of D_{int} may be associated with the interface magnetostriction [22].) It is to be regretted that [20] contains no further results that might enable us to check this hypothesis; so all we can do is to invite the experimentalists to proceed to further measurements on $Py_{300}/Cu_{50}/Py_{300}$.

Finally, it may be worth noting that our equation (31) can be rewritten in the form

$$J^{\text{AB}} = -a_0[(H_{\text{IM}} - H_{\text{UM}})/2D_{\text{ex}}]^{1/2} J_{\text{b}} \tag{32}$$

where $D_{\text{ex}} = 2A_{\text{ex}}/M$ is the exchange constant. Equation (32) shows that the greater D_{ex} in a given material, the better are conditions for the experimental observation of the IM peak.

Acknowledgments

The author is indebted to the Polish State Committee for Scientific Research for their support under Grant No 2 2361 91 02; he also wishes to thank Dr H Hurdequint (Université Paris-Sud) for his numerous discussions and for making accessible his experimental data prior to publication.

References

[1] Puszkarski H 1992 *J. Phys.: Condens. Matter* **4** 1595
[2] Puszkarski H 1992 *Phys. Rev.* B **46** 8926
[3] Puszkarski H 1992 *Phys. Status Solidi* B **171** 205
[4] Puszkarski H, Kołodziejczak B and Słomian M 1993 *J. Magn. Magn. Mater.* **121** 127
[5] Cracknell A P and Puszkarski H 1978 *Solid State Commun.* **28** 891
[6] Puszkarski H 1979 *Prog. Surf. Sci.* **9** 191
[7] Zhang P X and Zinn W 1987 *Phys. Rev.* B **35** 5219
[8] Hurdequint H and Dunifer G 1988 *J. Physique Coll.* **49** C8, 1717
[9] Krebs J J, Lubitz P, Chaiken A and Prinz G A 1989 *Phys. Rev. Lett.* **63** 1645
[10] Krebs J J, Lubitz P, Chaiken A and Prinz G A 1990 *J. Appl. Phys.* **67** 5920
[11] Parkin S S P, More N and Roche K P 1990 *Phys. Rev. Lett.* **64** 2304
[12] Guslienko K Yu, Lesnik N A, Mitsek A I and Vozniuk B P 1991 *J. Appl. Phys.* **69** 5316
[13] Heinrich B, Celinski Z, Myrtle K, Cochran J F, Arrott A S and Kirschner J 1991 *J. Magn. Magn. Mater.* **93** 75
[14] Yamazaki H, Ajiro Y, Hosoito N and Shinjo T 1991 *J. Phys. Soc, Japan* **60** 764
[15] Vohl M, Wolf J A, Grünberg P, Spörl K, Weller D and Zeper B 1991 *J. Magn. Magn. Mater.* **93** 403
[16] Mercier D, Lévy J C S, Watson M L, Whiting J S S and Chambers A 1991 *Phys. Rev.* B **43** 3311
[17] Fassbender J, Nörtemann F, Stamps R L, Camley R E, Hillebrands B, Güntherodt G and Parkin S S P 1992 *Phys. Rev.* B **46** 5810
[18] Puszkarski H 1970 *Acta Phys. Polon.* A **38** 217
[19] Heinrich B, Celinski Z, Cochran J F, Muir W B, Rudd J, Zhong Q M, Arrot A S and Myrtle K 1990 *Phys. Rev. Lett.* **64** 673
[20] Bosse H 1989 *PhD Thesis* Gesamthochschule Kassel-Universität, Kassel
[21] Hurdequint H private communication
[22] Szymczak H and Żuberek R 1993 *Acta Phys. Polon.* A **83** 651